Cairo University - Faculty of Engineering

Department of Electronics and

Communications Engineering

Antenna ELC 3050 Project

Dual – Polarized Microstrip Patch Antenna operating at 28GHz

Under Supervision of Prof: ***Islam A. Eshrah***

Name	*Sec*	*BN*	*I D*
Farouk Hashem Saed	**3**	**17**	**9210798**
Mohamed Ali Ali El-Naggar	**4**	**2**	**9213341**
Ahmed Adel Younes Sayed Ahmed	**1**	**16**	**9213073**
Ahmed Amr Tawfik Abdelghaffar	**1**	**20**	**9210112**
Ahmed Mohamed Fergany Dardiry	**1**	**24**	**9210144**
Ali Ahmed Mohamed Ahmed	**2**	**52**	**9210666**

Dual-Pol Microstrip Patch Antenna operating at 28 GHz.

Abstract – This paper presents the design of a 28GHz, dual-polarized, microstrip patch antenna. The study focuses on designing, simulating the chosen design to address challenges in millimeter-wave frequencies, includes an in-depth investigation of electromagnetic characteristics, considering impedance matching, polarization isolation, and radiation patterns and explores the effect of each design parameter on the expected results. Simulation studies optimize the design, and extensive measurements validate its feasibility. Results indicate the effectiveness of the proposed dual-polarization antenna at 28 GHz, with tool verifications to ensure the validity of the results in real-world scenarios.

1. Framework

1.1 Introduction

Microstrip patch Antenna (MSA) has played a pivotal role in the evolution of wireless communication, spanning a rich history of technological advancements. The continual demand for higher data rates, increased capacity, and improved spectral efficiency has driven antenna engineers to explore innovative solutions. In this context, dual-polarization antennas have emerged as a promising avenue for enhancing communication systems. Dual-polarization antennas offer the advantage of transmitting and receiving signals in both horizontal and vertical polarizations simultaneously. This capability is particularly relevant in modern wireless communication systems due to their potential to mitigate multipath fading, improve channel capacity, and enhance overall system performance. The applications of dual-polarization antennas span a wide range, including point-to-point communication, satellite communication, radar systems, and 5G networks. The choice of operating frequency is a crucial consideration in antenna design. The focus on 28 GHz is driven by the increasing interest in millimeter-wave bands for 5G communication. The 28 GHz frequency band offers a significant bandwidth, allowing for higher data rates and increased capacity. As 5G networks continue to evolve, the deployment of antennas operating at higher frequencies becomes essential to meet the growing demand for data-intensive applications. However, the design of antennas at 28 GHz and beyond poses unique challenges. At these frequencies, the effects of atmospheric absorption, signal blockage, and increased free-space path loss become more pronounced. Additionally, the integration of dual-polarization capabilities introduces complexities in terms of design, impedance matching, and isolation between polarizations. These challenges necessitate a comprehensive understanding of the electromagnetic behavior at millimeter-wave frequencies and innovative design approaches.

1.2 Problem Definition

Feeding Mechanism: *The patch antennas may be powered with many methods. The processes feeding is categorized in two methods:*

- *In category contacting, the feeding technique is powered by means of a connecting element such as a microstrip line into the radiating patch.*
- *Without contact category, a transfer of power between the microstrip line and radiating element is performed with the electromagnetic field coupling.*

Each feeding mechanism has its advantages and limitations, and antenna engineers select the most appropriate one for a particular application based on these considerations.

Dual Edge - Fed Microstrip Patch Antenna:

In this kind of feeding process (Fig.1), the edge of the microstrip patch is connected directly to a conducting strip. This feeding method offers the benefit that the conducting line can have the opportunity of engraved on same substrate of patch antenna providing a planar shape. The width of the conducting element is smaller as compared to the patch antenna.

Main design specification that must be considered:

- ***Port matching***

- ***Isolation between the two feeding ports*** *in a dual-polarized antenna is crucial to ensure that the signals intended for one polarization do not interfere with the signals of the orthogonal polarization. Differential feeding-based topologies and external self-interference cancellation (SIC) mechanisms can be used to achieve additional isolation. [1]*

- ***XPD (Cross-Polarization Discrimination)*** *defines the ability of an antenna to discriminate against signals with a polarization different from the intended polarization. XPD quantifies the level of isolation between the co-polarized (intended) and cross-polarized (unintended) components.*

  Several factors can affect the isolation between the two feeding ports and XPD:

  - *Physical Separation & Feed System*
  - *Feeding Network Design*
  - *Geometry & Material Properties*

2. Design Procedure

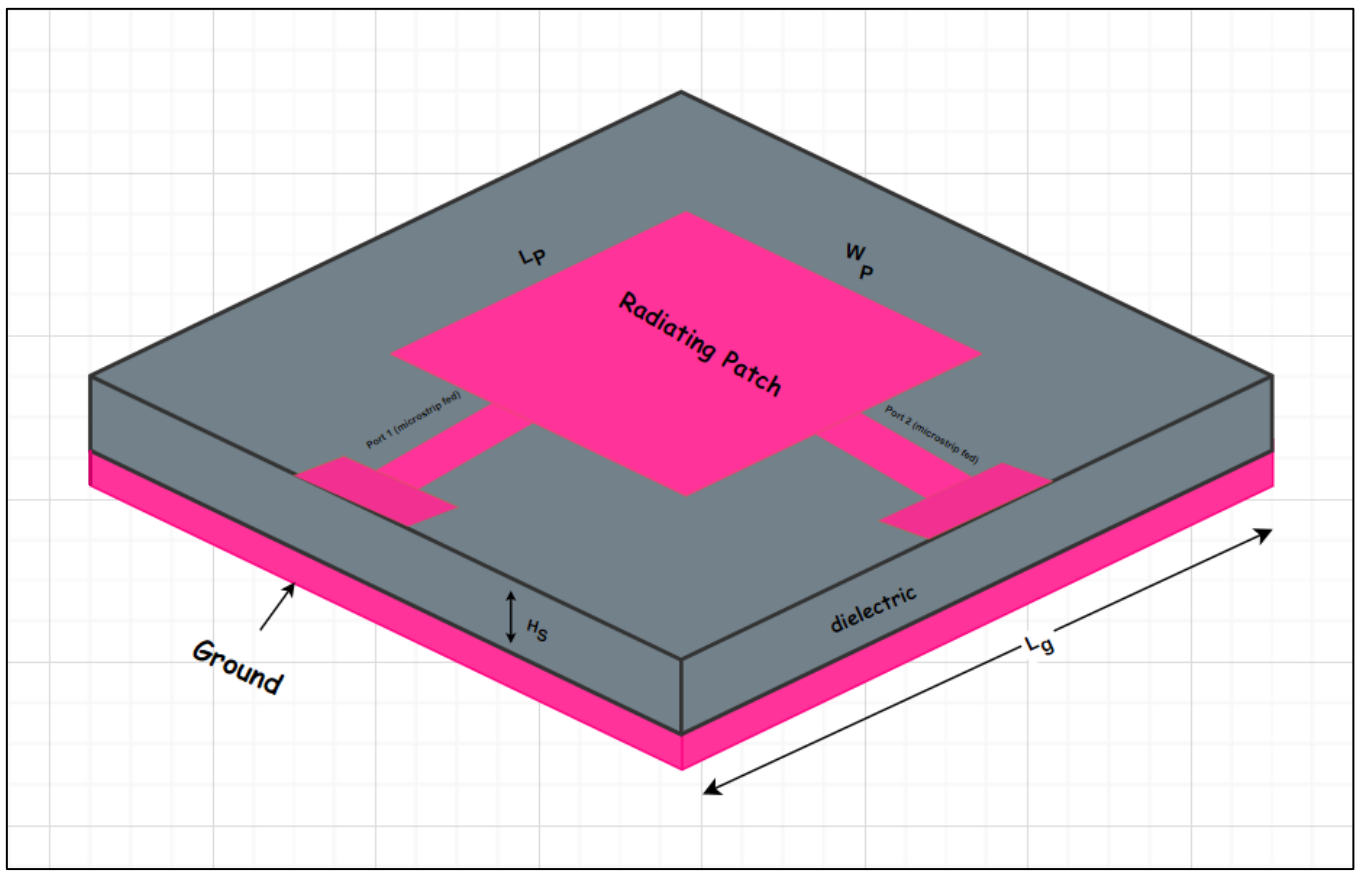

Figure 1: Design Figure

- *Conductive surfaces are made of copper (thickness = 50 um)*
- *Substrate is made of Roger 4003:* $\epsilon_r = 3.55, \tan\delta = 0.0027$

2.1 Antenna Modeling

- ***Fringing effect:***

In Figure (3) shown below, the microstrip patch antenna is represented by two slots, separated by a transmission line of length L and open circuited at both the ends. Along the width of the patch, the voltage is maximum, and current is minimum due to the open ends. The fields at the edges can be resolved into normal and tangential components with respect to the ground plane. It is seen from Figure 2 that the normal components of the electric field at the two edges along the width are in opposite directions and thus out of phase since the patch is λ/2 long and hence they cancel each other in the broadside direction. The tangential components (seen in Figure 2), which are in phase, means that the resulting fields combine to give maximum radiated field normal to the surface of the structure [2]. Due to the effect of fringing, a microstrip patch antenna would look electrically wider compared to its physical dimensions. As shown in Figure 2, waves travel both in substrate and in the air. Thus, an effective dielectric constant ε_{reff} is to be introduced. The effective dielectric constant ε_{reff} takes into account both the fringing and the wave propagation in the line. Radiation from the edges of the patch can affect the radiation pattern and may lead to undesired side lobes. [3]

Initial design dimensions introduced below based on ideal conditions are later tuned and optimized to compensate for the non-idealities.

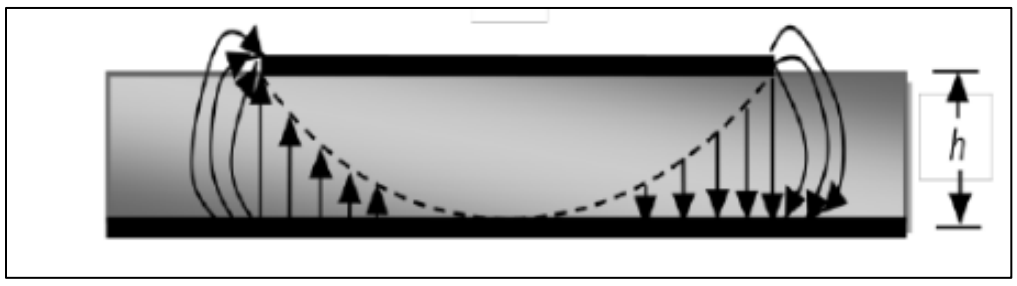

Figure 2: Fringing fields

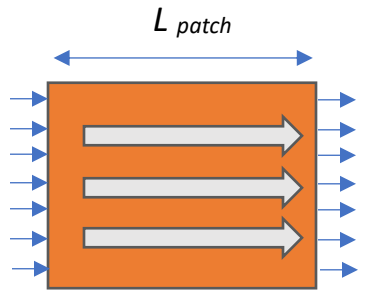

Figure 3: Top view & surface currents

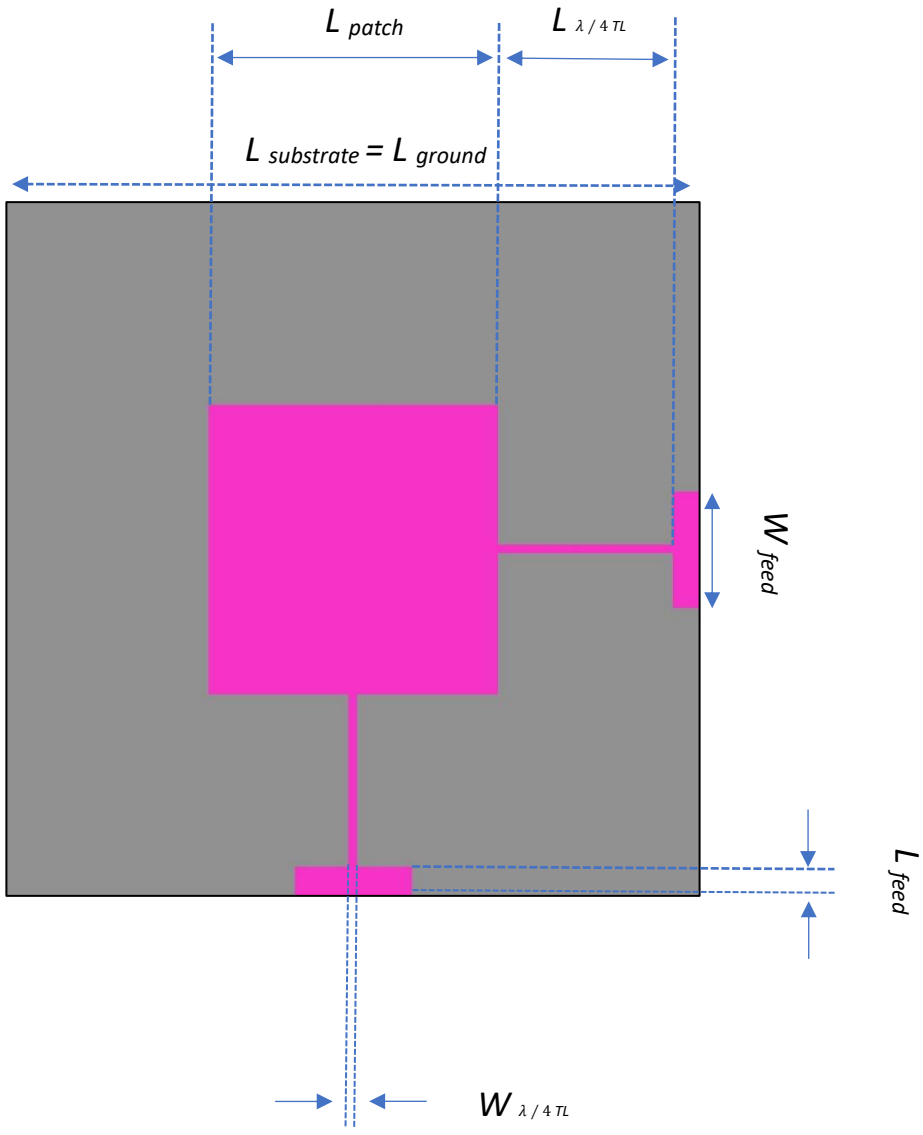

2.2 Design parameter equations and Values:

Dimension	***Equation***	***Tuned Value (mm)***
ε_{reff} *(fringing)*	$\frac{\varepsilon_r+1}{2}+\frac{\varepsilon_r-1}{2}*\frac{1}{\sqrt{1+12\left(\frac{H_S}{W}\right)}}$	-
λ_{eff}	$\frac{\lambda_o}{\sqrt{\varepsilon_{eff}}}$	-
ΔL (fringing)	$\frac{(\varepsilon_r-0\cdot3)\left({}^{W}/_{H_s}+0.264\right)}{(\varepsilon_r-0\cdot298)\left({}^{W}/_{H_s}+0.8\right)}$	-
$H_{substrate}$	${}^{\lambda_s}/_{20}<H_s<{}^{\lambda_s}/_{4}$	*0.5*
$L_{substrate} = L_{ground}$	$L_{patch} + 6\,H_s$	*7*
$L_{patch} = W_{patch}$	$W=\frac{\lambda_s}{2}\sqrt{\frac{2}{\varepsilon_r+1}}$	*2.482*
$Z_{in\text{-}patch}$	$90\frac{\varepsilon_r^2}{\varepsilon_r-1}\left(L_p/W_p\right)^2 = 444.794\ \Omega$	-
$Z_{\lambda/4\,TL}$	$\sqrt{Z_0*Z_{in}} = 149.13\ \Omega$	-
$L_{\lambda/4\,TL}$	$L=\frac{\lambda_{eff}}{4}$	*2*
$W_{\lambda/4\,TL}$	$Z_o\approx\frac{60}{\sqrt{\varepsilon_r}}\ln\left(\frac{8H_s}{W_{TL}}+\frac{W_{TL}}{4H_s}\right)$	*0.1127*
L_{feedTL}	$L_{ground} - L_{patch} - 2\,L_{\lambda/4\,TL}$	*0.259*
W_{feedTL}	$Z_o\approx\frac{120\pi}{\sqrt{\varepsilon_r}\left(\frac{W_{TL}}{H_s}+1.393+0.667*\ln\left(\frac{W_{TL}}{H_s}+1.44\right)\right)}$	*1.1184*
Patch, Ground and TL Thickness	*0.05*	*0.05*

Table 1: Parameter Equations

3. Results and Discussion

CST 3D EM analysis tool was used to simulate and test the antenna model

I. Return Loss of the antenna ($|S_{11}|$ &$|S_{22}|$)

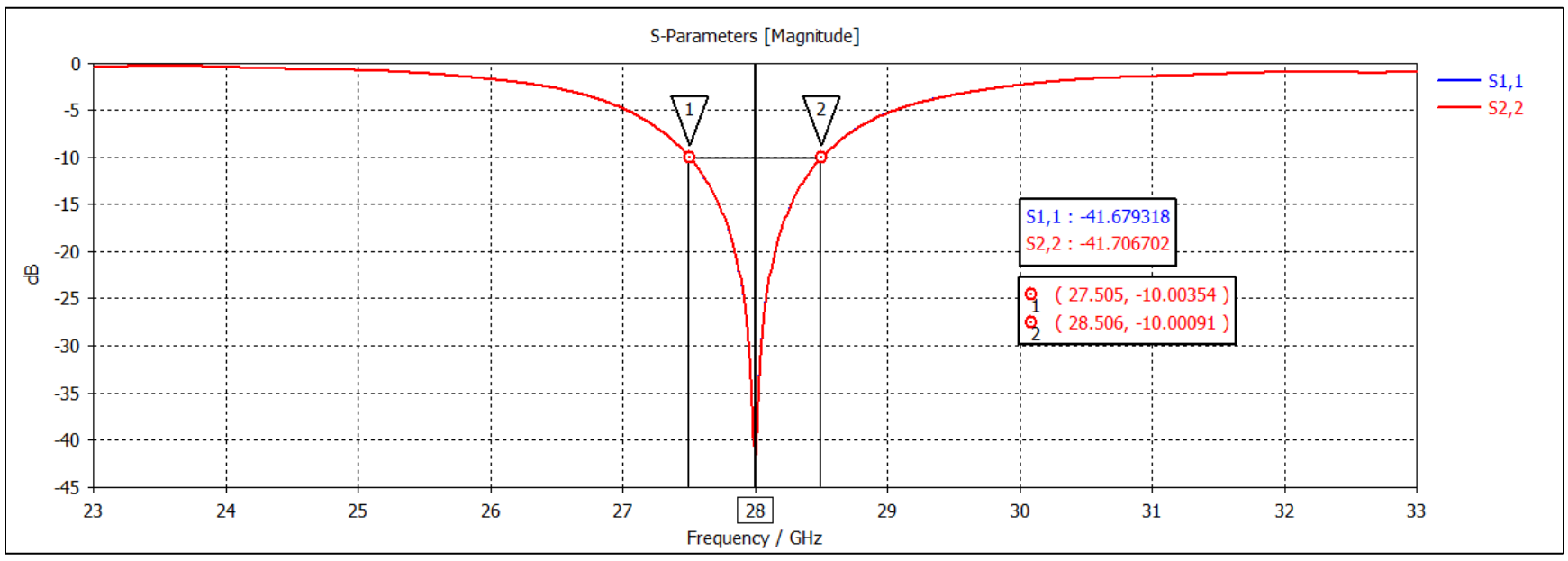

Figure 4: S11, S22

The Return loss of the antenna measures how much power is delivered to the antenna at different frequencies and its matching. Designing the antenna to radiate at 28GHz, we achieved a return loss of - 41.7 dB. results are shown in figure 4 (BW = 1GHz = 3.6%)

II. Coupling between the two ports ($|S_{21}|$)

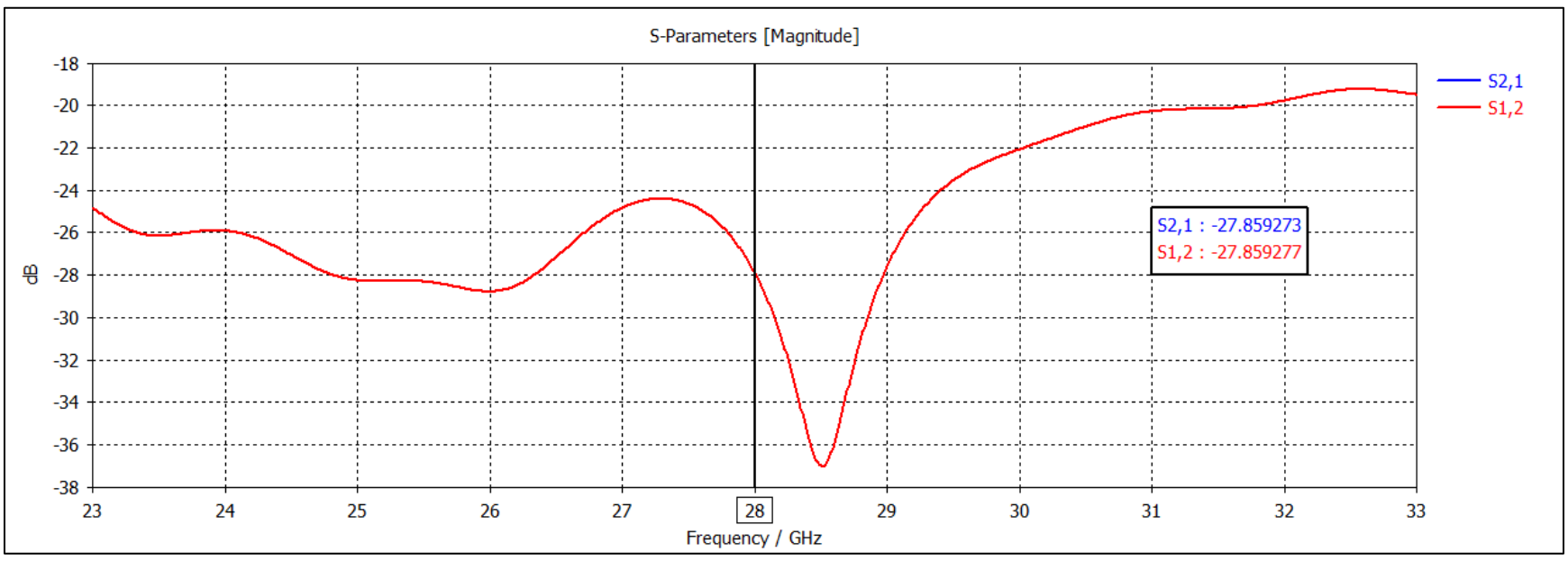

Figure 5: S21, S12

Coupling between the two ports indicates how power is reflected between the two ports and how the ports affect each other at 28GHz we got S_{21} of – 27.86 dB, Figure 5 shows how S_{21} changes against frequency.

III. 1] The input impedance of the antenna on the smith chart

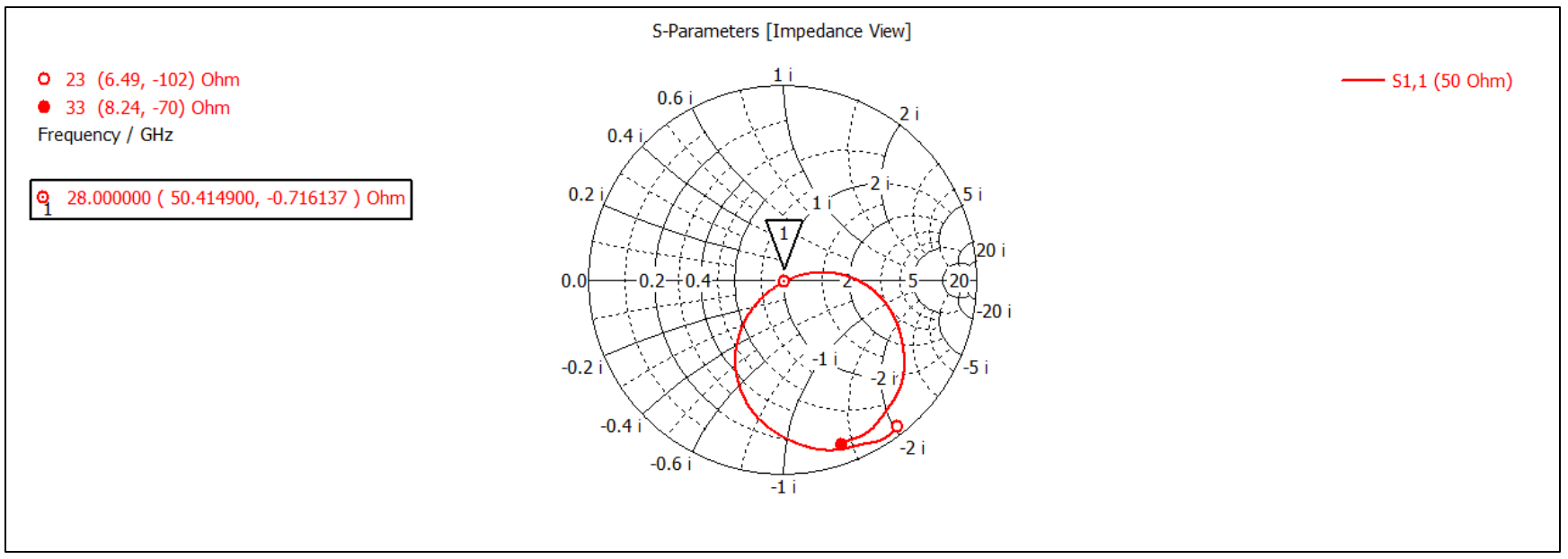

Figure 6: Zin smith chart

The input impedance of the antenna looking from the port is shown in figure 6 and the input impedance of the radiating patch after de-embedding the source reference plane to the edge of the antenna is shown in a linear plot in figure 7 and on the smith chart in figure 8.

2] De-embedding

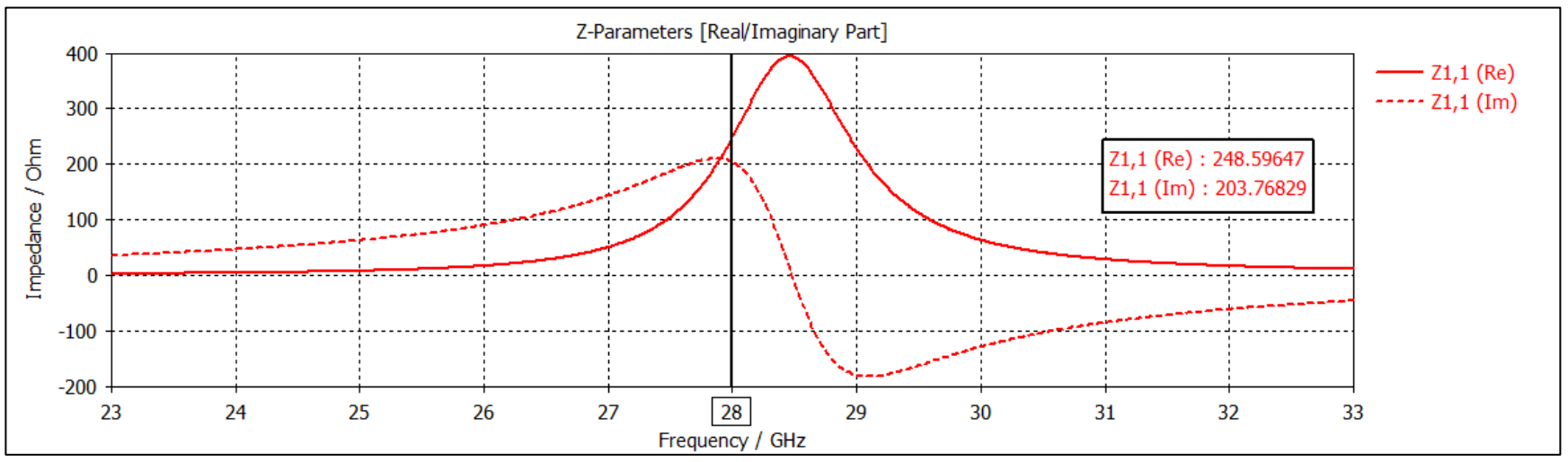

Figure 7: Zin smith chart

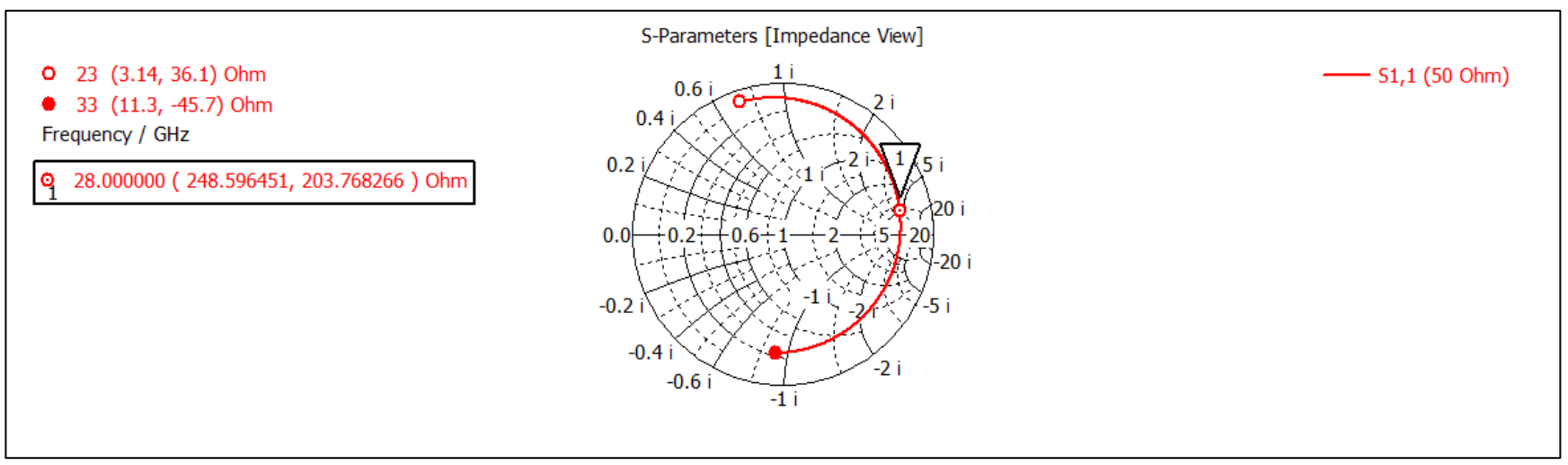

Figure 8: Zin smith chart

IV. The radiation pattern (c-pol & cross-pol) in E-Plane & H-Plane and XPD

1] E – plane (the plane having the direction of maximum radiation (Z-axis) and the feeding direction)

Port1 => Feeding (Y-axis)
Port2 => terminated

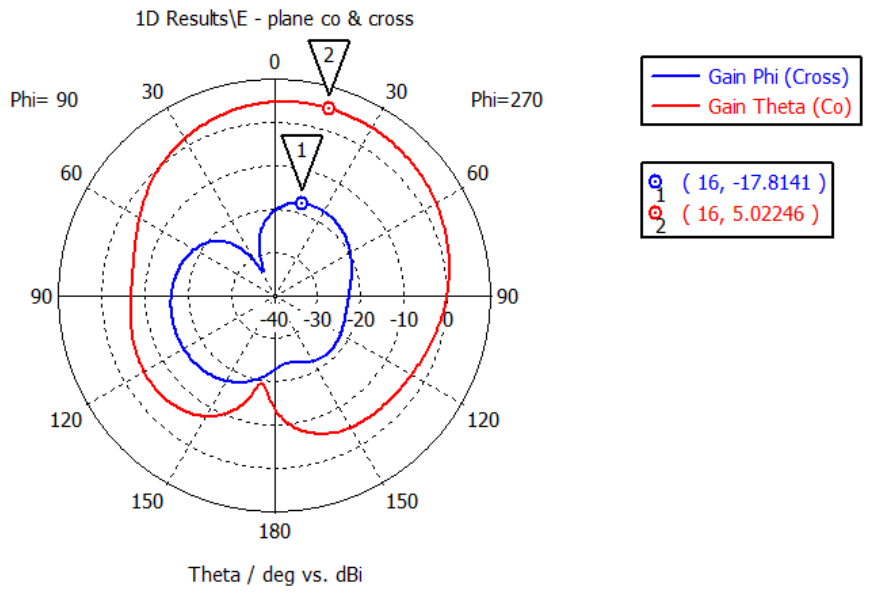

Figure 9: Gain Co & Cross

$$XPD\ (E-plane) = G_{co} - G_{cross} = 5.02246 - (-17.8141) = 22.83656\ dB$$

2] H – plane (the plane having the maximum radiation direction and the direction perpendicular to the feed direction)

Port1 => Feeding (Y-axis)
Port2 => terminated

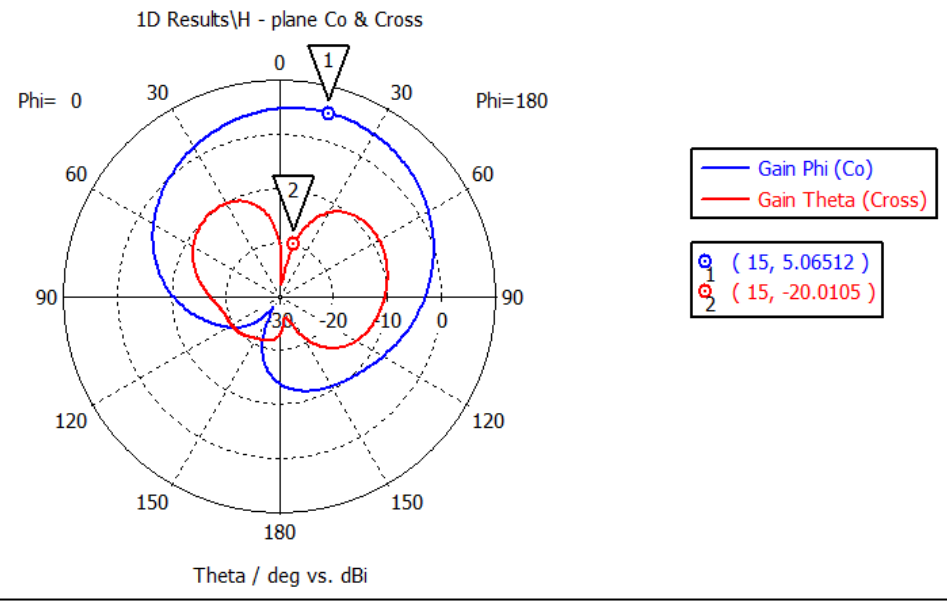

Figure 10: Gain Co & Cross

$$XPD\ (H-plane) = G_{co} - G_{cross} = 5.06512 - (-20.0105) = 25.07562\ dB$$

For a dual polarized antenna there are two sources, so with enabling one source at a time, the radiation patterns achieved are shown in figure 9 & figure 10. note that for each source E-Plane and H-Plane switch, because of the symmetry and reciprocity of the design. Same applies when measuring the XPD of the antenna.

V. The gain & radiation efficiency of the antenna vs frequency

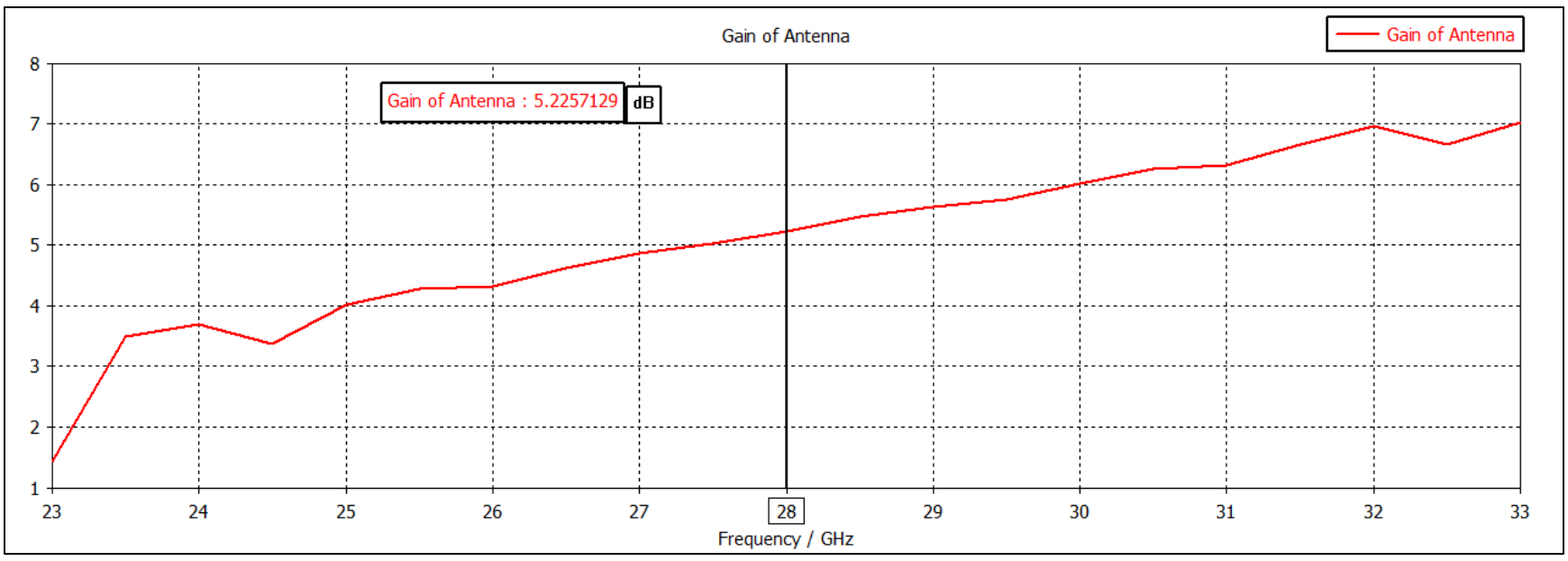

Figure 11: Antenna Gain

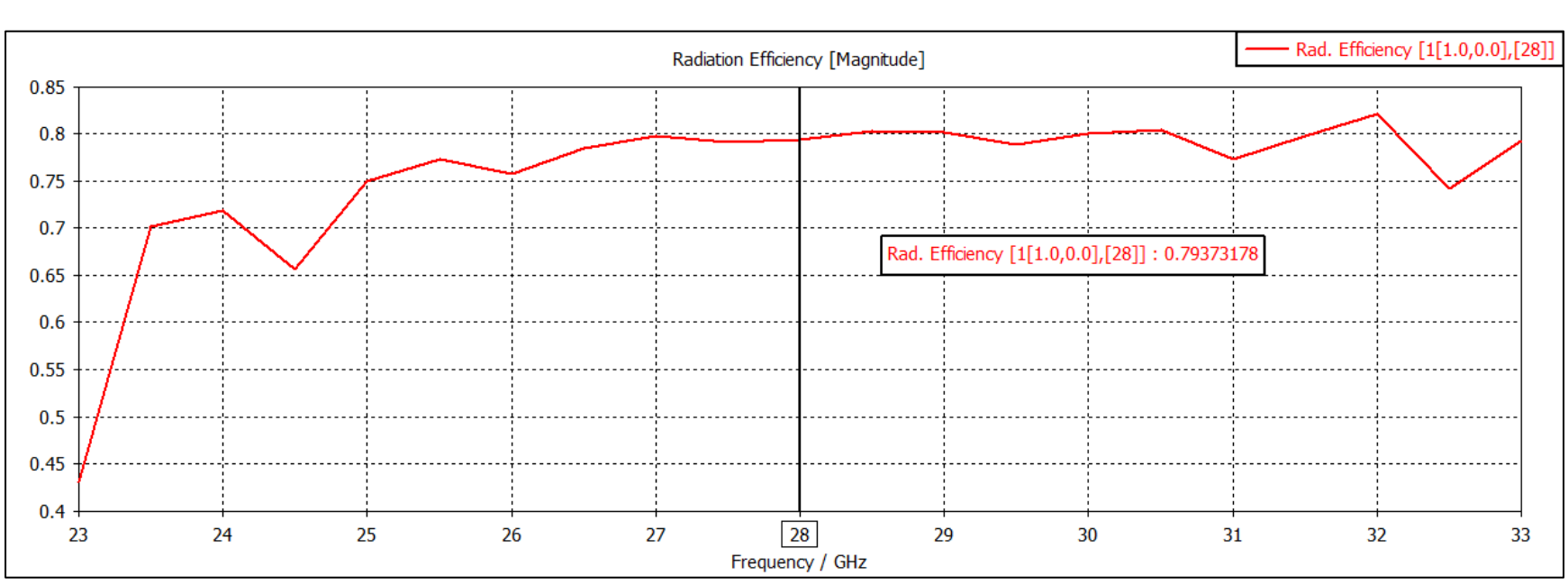

Figure 12: Radiation Efficiency

Gain and Radiation Efficiency of the antenna are important parameters to measure the power efficiency of the antenna and how well it "spreads" or "directs" its radiated power. At the intended frequency, our design achieved a gain of 5.226 dB in broadside direction and a radiation efficiency of 79%. Figure 11 & figure 12 show how these parameters change with frequency.

4. Final Design Layout

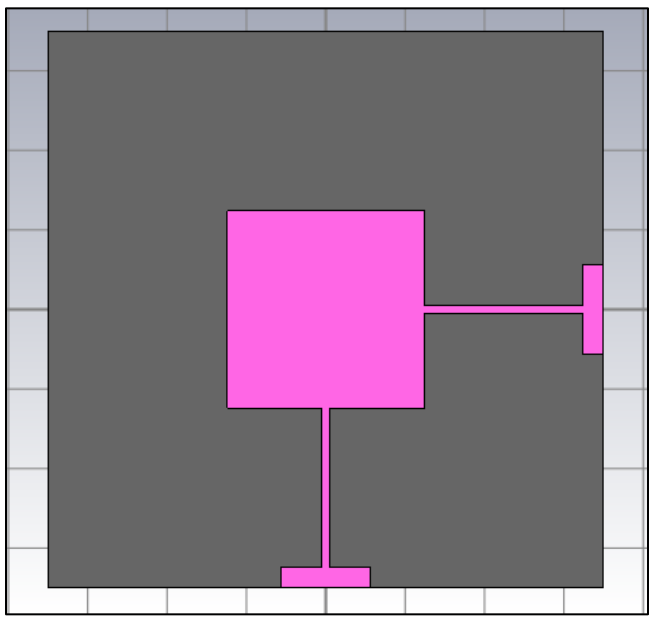

Figure 13: Top view

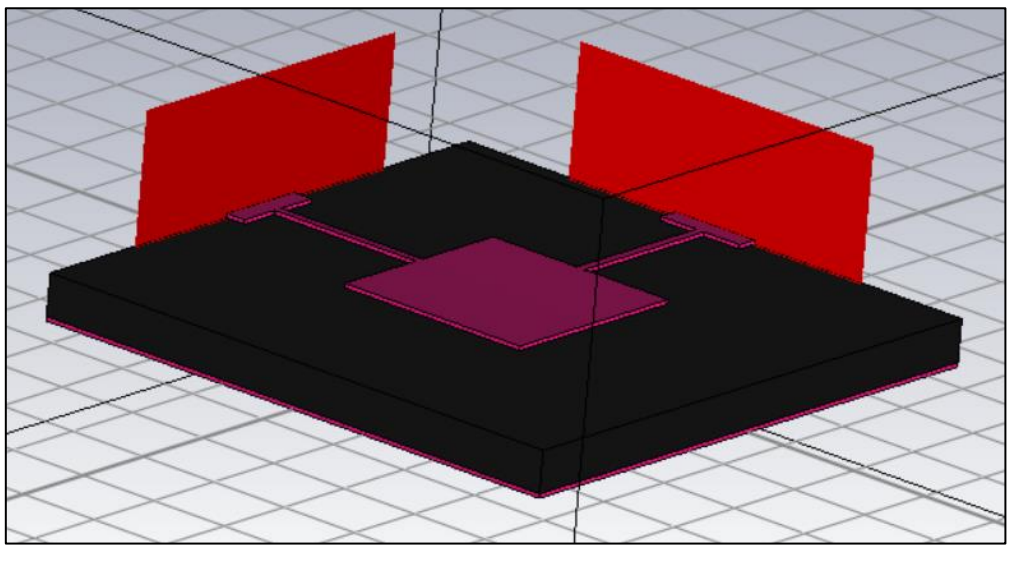

Figure 14: Isometric View

Final Parameters List (mm):

Patch	***2.482 x 2.482***
λ / 4 TL	***2 x 0.1127***
Feed	***0.259 x 1.1184***
Conductor	***Copper Thickness = 0.05***
Substrate	***Roger 4003 7 x 7 x 0.5***

Table 2: Design Parameters

Achieved Specs:

Return Loss	***- 41.7 dB***
Port to port isolation	***- 27.86 dB***
Gain	***5.23 dB***
Radiation Efficiency	***79%***
XPD (E - plane)	***22.84 dB***
XPD (H – plane)	***25.076 dB***

Table 3: Antenna Specifications

5. *Equivalent Circuit Model (using ADS)*

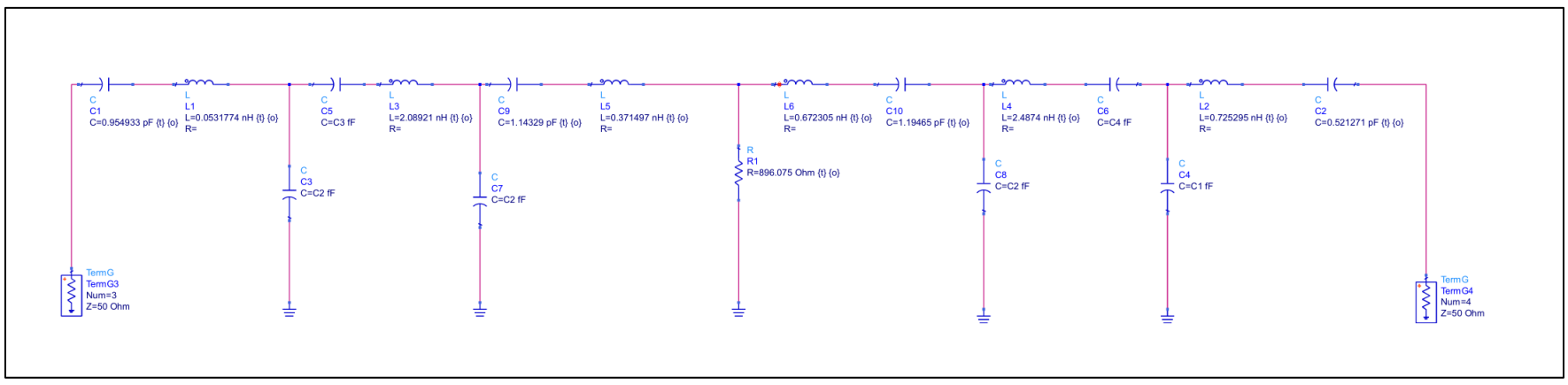

Figure 15: ADS schematic

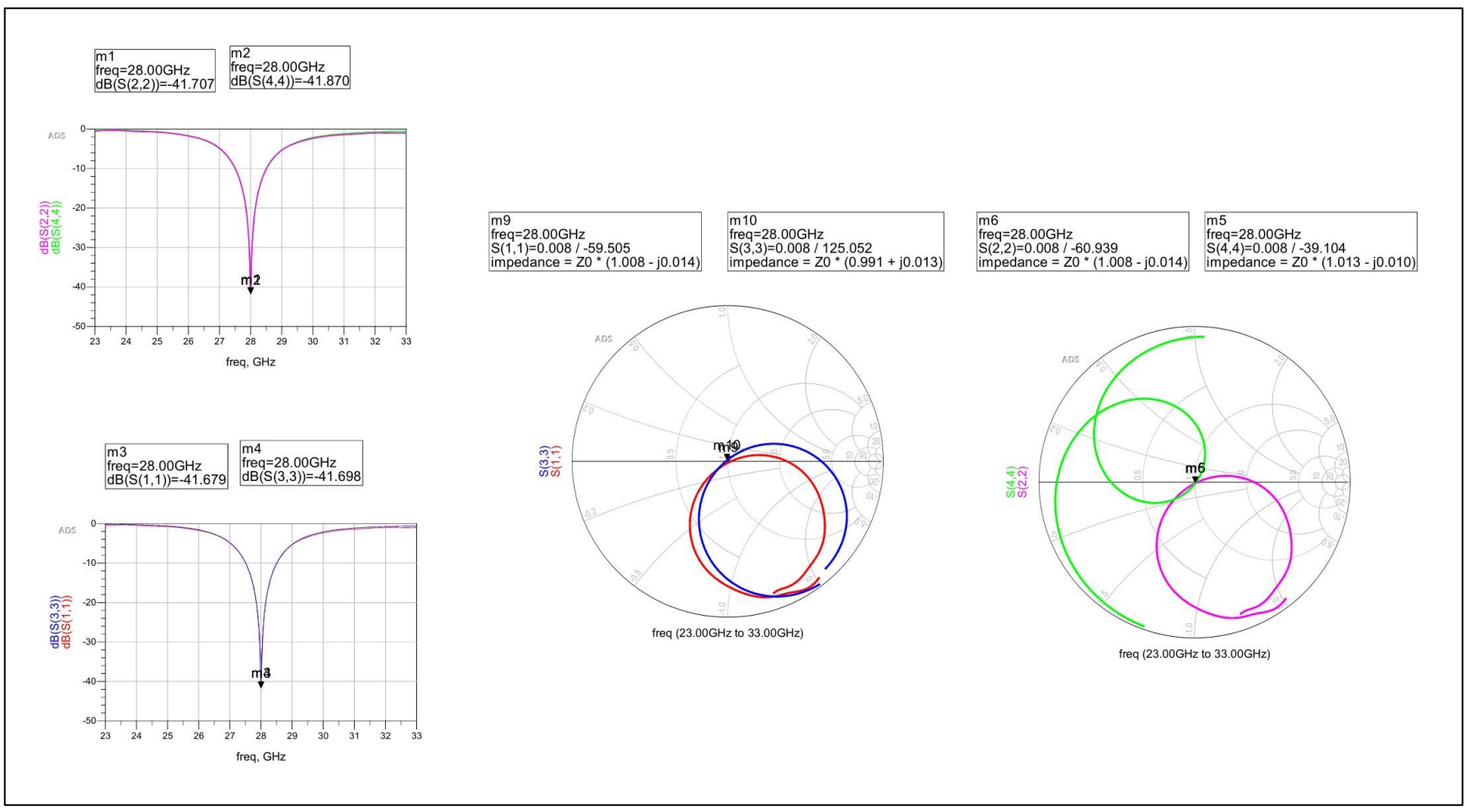

Figure 16: ADS Results

6. Tool Verification:

In this section we will introduce a simulation for a fabricated dual-polarized 2.4 GHz square-shaped patch with two perpendicularly placed thin co-planar quarter-wave feeds made with 1.6 mm thick FR-4 substrate (ϵr = 4.4, tan δ = 0.02).
This fabricated antenna was introduced in this paper: Nawaz H, Niazi AU. Characterization of dual-polarized monostatic patch antennas for full-duplex applications. Engineering Reports. 2020; 2:e12180. https://doi.org/10.1002/eng2.12180

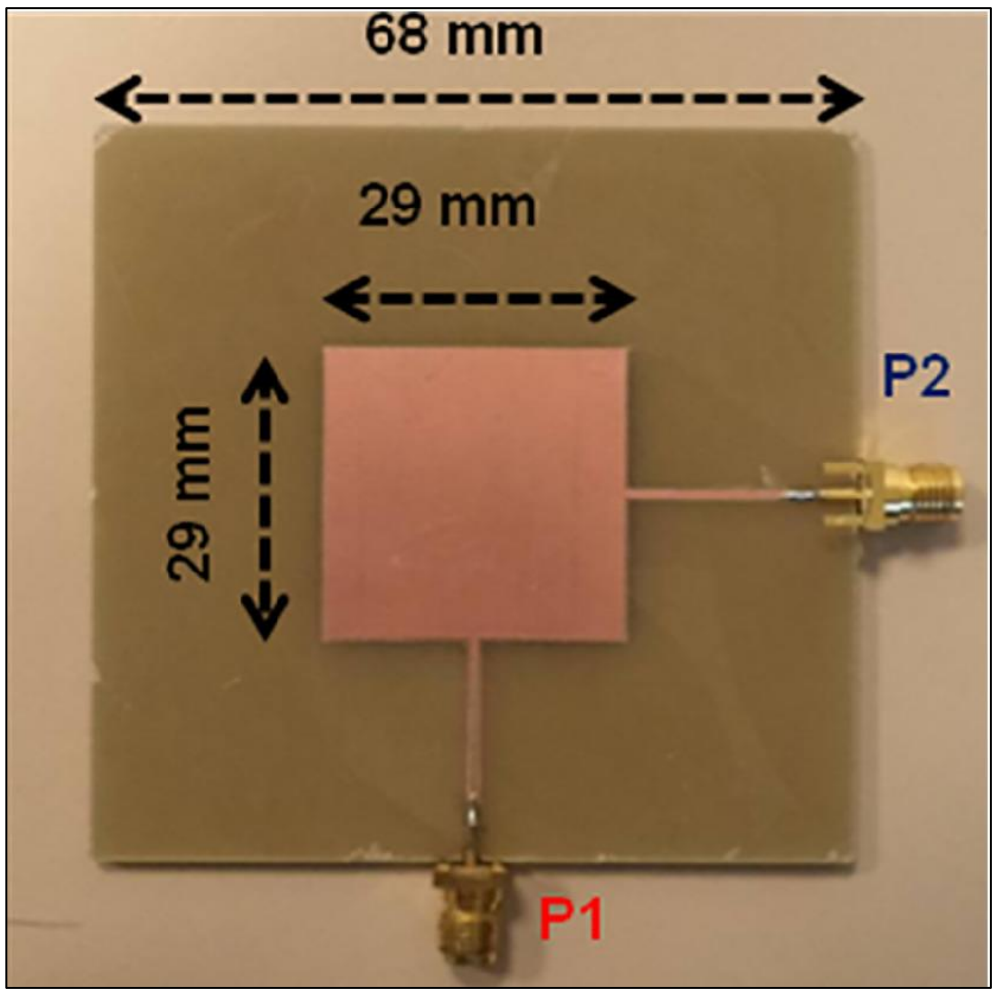

Figure 17: Report Fabricated Antenna

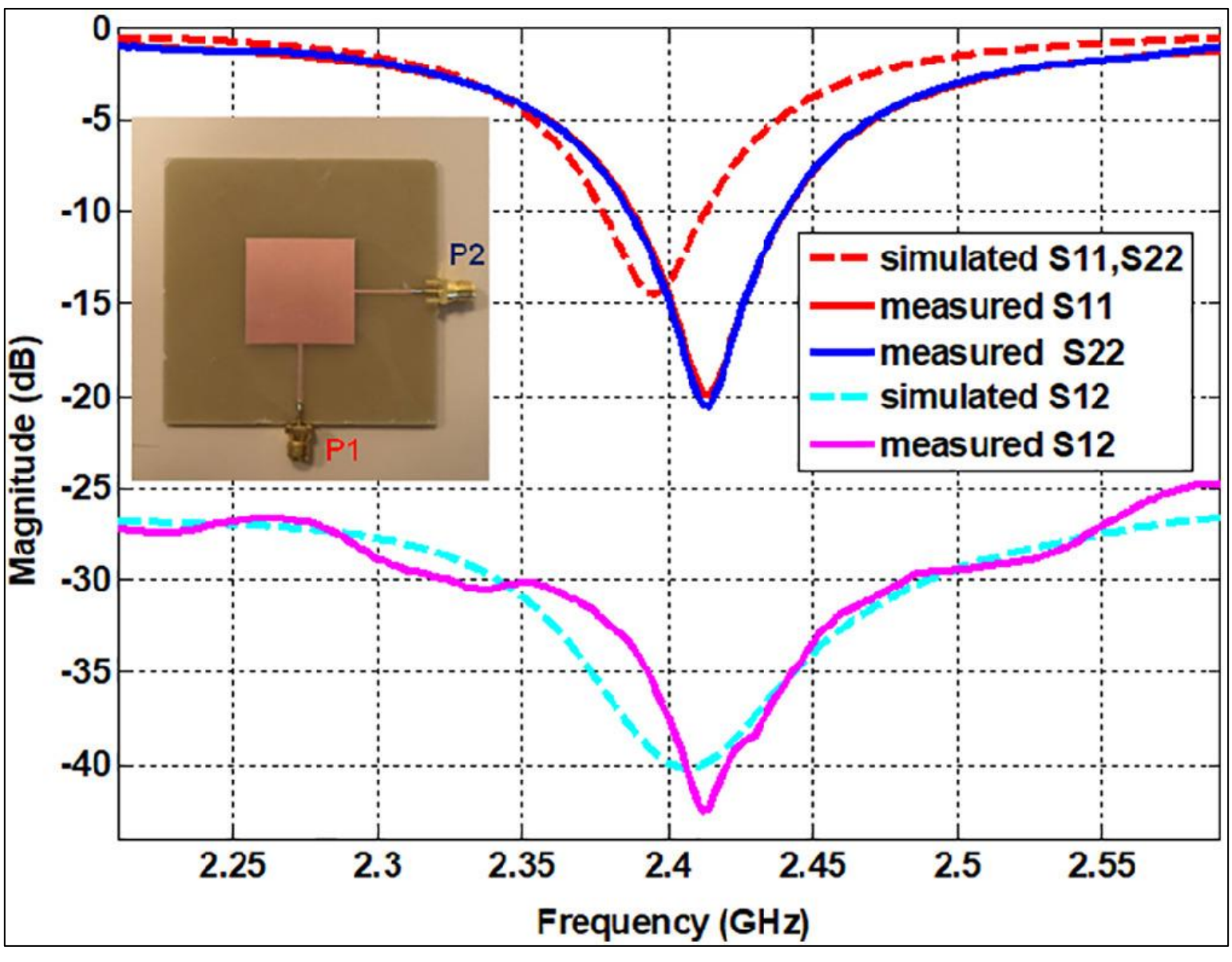

Figure 18: Report Lab Measured Results

CST Verification:

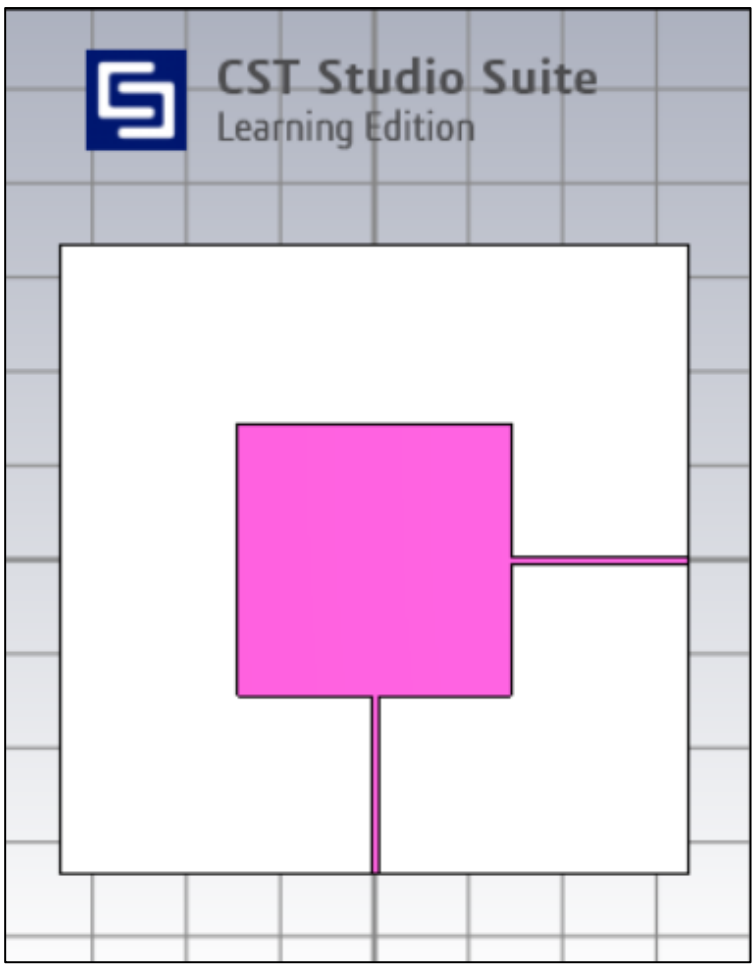

Figure 19: Our Replicated design

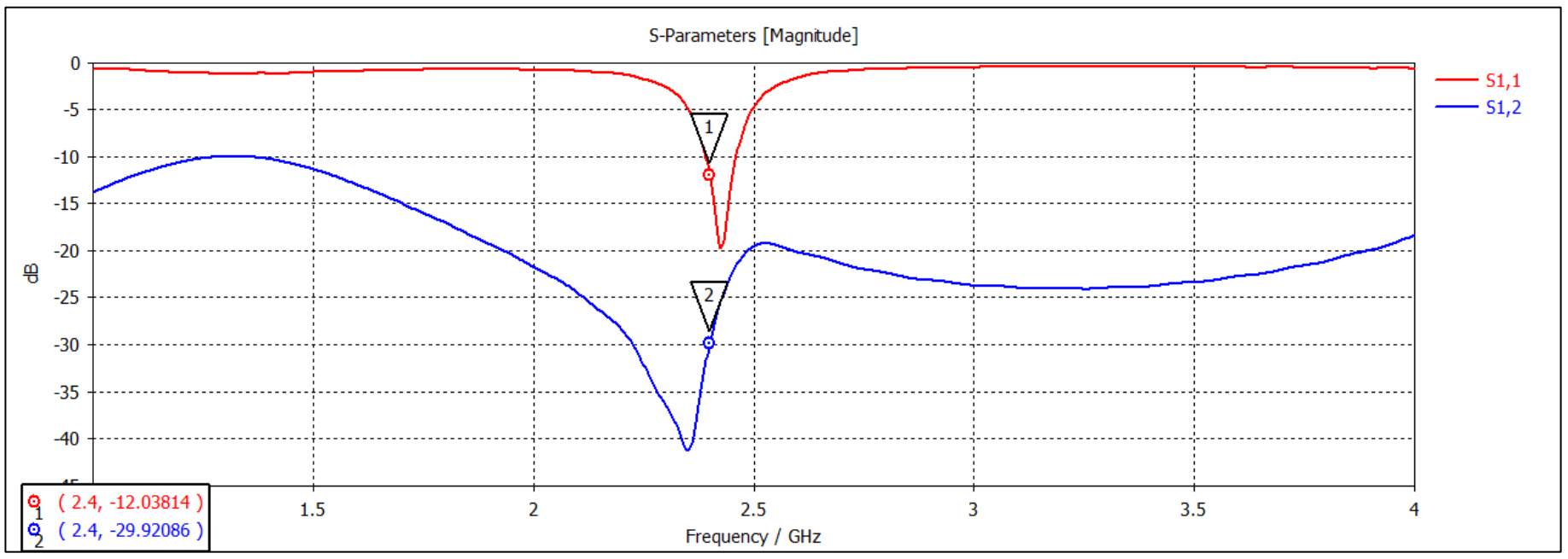

Figure 20: Simulation Results

	E5062A RF Network Analyzer	**CST**
S11, S22	*- 20 dB*	- 12 dB
S21, S12	- 42 dB	-30 dB

Table 4: Comparison

To verify the accuracy of our simulation results and ensure their alignment with the findings presented in the referenced paper, a comprehensive validation process was undertaken. Firstly, we replicated the simulation setup described in the paper, including the antenna geometry, substrate properties, and feed network configuration. We utilized the same simulation tools (CST), ensuring consistency with the methodology outlined in the referenced paper. Following the simulations, a thorough analysis of key antenna parameters such as return loss, gain, and radiation patterns was conducted.

The obtained results were then compared with the published lab measured data from the reference paper. Close attention was paid to the measured Tx-Rx port to port isolation and return loss to ascertain that our simulation outcomes closely matched those reported in the paper. We carefully looked for any differences or changes and kept adjusting the simulation settings until we got a good match.

7. Conclusion

In summary, the development and assessment of our dual-port microstrip patch antenna, employing an edge-feed configuration with a quarter-wave transformer, have yielded promising outcomes at the central frequency of 28 GHz. With a gain of 5.23 dB and an impressive return loss of -41.7 dB, the antenna exhibits effectiveness in minimizing reflected signals and optimizing power transfer.

The notable feature of port-to-port isolation, achieving -27.86 dB, underscores the antenna's success in mitigating mutual coupling between its ports. The observed radiation efficiency of 79% further accentuates the antenna's ability to efficiently convert input power into radiated energy, contributing to its overall power efficiency.

Significantly, cross-polarization discrimination emerges as a strength, with the antenna achieving 22.84 dB in the E-plane and 25.076 dB in the H-plane. This capability ensures the maintenance of polarization purity and a critical factor for effective communication at higher frequencies.

In practical terms, the designed dual-port microstrip patch antenna with an edge-feed configuration and a quarter-wave transformer stands out as a reliable and efficient solution for high-frequency applications at 28 GHz. Its strong performance across key parameters positions it as a valuable component for scenarios demanding optimal power efficiency, directed radiation, and minimal interference at 28 GHz.

8. References

[1] Nawaz, H. and Tekin, I. (2016), Dual port single patch antenna with high interport isolation for 2.4 GHz in-band full duplex wireless applications. Microw. Opt. Technol. Lett., 58: 1756-1759. https://doi.org/10.1002/mop.29899

[2] C. A. Balanis, "Antenna Theory, Analysis and Design," John Wiley & Sons, New York, 1997.

[3] Elrashidi, Ali & Elleithy, Khaled & Bajwa, Hassan. (2011). The fringing and resonance frequency of cylindrical microstrip printed antenna as a function of curvature. EURASIP Journal on Wireless Communications and Networking. 3.

[4] D. M. Pozar and D. H. Schaubert, Microstrip Antennas: The Analysis and Design of Microstrip Antennas and Arrays, Wesley Publications

[5] Soliman, M. M., Hakim, M. L., Uddin, M. J., Faisal, M. M. A., & Rahaman, A. (2019). Optimization of Design Parameters of Microstrip Patch Antenna at 28 GHz and 38 GHz for 5G Applications. 2019 IEEE International Conference on Telecommunications and Photonics (ICTP). doi:10.1109/ictp48844.2019.904177